Synthesis, Properties, and Polymerization of New Liquid Crystalline Monomers for Highly Ordered Guest−Host Systems

Rafael Piñol,[†] Johan Lub,[‡] Maria Pilar García,[†,‡] Emiel Peeters,[‡] José Luis Serrano,[†] Dirk Broer,[‡] and Teresa Sierra[†,*]

Instituto de Ciencia de Materiales de Aragón, Química Orgánica, Facultad de Ciencias, Universidad de Zaragoza-CSIC, 50009 Zaragoza, Spain, and Philips Research, High Tech Campus 11, 5656AE Eindhoven, The Netherlands

The present study is aimed at the preparation of highly ordered guest−host systems based in liquid crystalline materials with potential application in the preparation of thin film polarizers. To accomplish this purpose, we carried out the design, synthesis, and mesomorphic characterization of new reactive liquid crystalline monomers. All the compounds exhibited liquid crystalline behavior. The effect of structural variations on the mesomorphic properties was investigated. The existence of a highly ordered lamellar phase (S_B) within the mesomorphic behavior of the reactive monomers was confirmed by polarized optical microscopy (POM) and X-ray diffraction (XRD) techniques. Four series of photopolymerisable dichroic mixtures including a dye (**G205**) and different percentages of the liquid crystal monomers were prepared. The dichroic ratio *DR* and order parameter *S* of the dye in the different liquid crystal matrixes were determined by polarized UV−vis spectroscopy in aligned samples. In situ photopolymerization of the liquid crystalline mixtures at room temperature in the highly ordered S_B phase resulted in the formation of cross-linked polymeric networks in which the anisotropic absorption of the film was fixed. High dichroic ratio values, exceeding 50, were measured for some of the anisotropic networks. The thermal stability of the anisotropic films obtained was also studied.

Introduction

Enhancement of the optical performance of liquid crystal displays (LCDs) requires a number of optical films added to the optical path of the LCD. Typically, these films include polarizers, diffusers, compensation films and brightness enhancing films. New research is focused on the development of ultrathin integrated optical films with a typical thickness of around 1 or 2 μm.[1] The optical components under investigation are polarisers, retarders with a uniaxial (planar), tilted or splayed orientation,[2] diffusers and color filters[3] based on cholesteric liquid crystals with several integrated optical functions in a single layer. These advanced optical films, much thinner than the traditional optical components, can be included as part of the structure of a liquid crystal cell (incell components). Thus, the thickness of an LCD can be reduced from ∼100 μm per film using traditional optical components to 1−2 μm when using incell optical components. The exterior of the display is now formed by the glass substrates, which gives a higher scratch resistance, whereas a reduction in the final weight of the display can also be achieved. Moreover, these new thin in-cell components may play a role in the development of flexible displays,[4] because
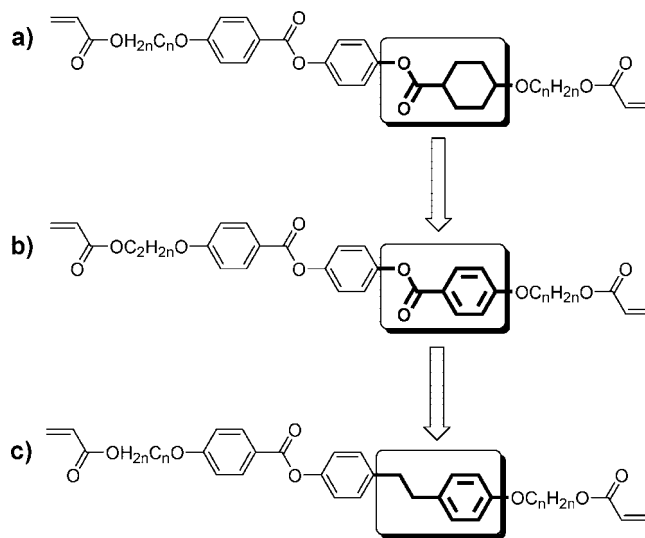
Figure 1. Schematic outline of the design process followed in this study remarking the structural changes considered to ensure ordered smectic behavior. (a) Chemical structure of the liquid crystalline diacrylates derived from cyclohexane carboxylic acid.[6] (b) Core with three aromatic rings that would simplify the synthetic procedure, but promotes nematic and smectic-A behavior.[13] (c) General structure of the three ring core designed to fulfill the material requirements for the present study.

for incell component displays, the optical properties of the substrates become less critical, which allows for a number of additional degrees of freedom in the optical design of LCDs.[5]

In a previous publication,[6] a new approach to thin film polarizers for incell application in LCDs was reported. It was based on highly ordered guest−host systems by in situ

* To whom correspondence should be addressed. E-mail: tsierra@unizar.es.
† Universidad de Zaragoza-CSIC.
‡ Philips Research.

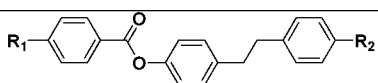(1) Lub, J.; Broer, D. J.; Wegh, R. T.; Peeters, E. *Mol. Cryst. Liq. Cryst.* **2005,** *429,* 77.
(2) Seiberle, H.; Benecke, C.; Bachels, T. *SID Dig.* **2003,** 1162.
(3) Hochbaum, A.; Jiang, Y.; Li, L.; Vartak, S.; Faris, S. *SID Dig.* **1999,** 1063.
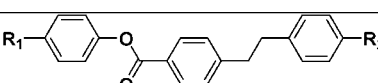(4) Sergan, T.; Schneider, T.; Kelly, J.; Lavrentovich, O. D. *Liq. Cryst.* **2000,** *27,* 567.

Chart 1. General Structure

Comp.	R_1	R_2	Phase Transitions (°C) [kJ/mol][a]
A_1	$CH_2=CH-COO-C_6H_{12}O-$	$-OC_6H_{12}-OOC-CH=CH_2$	Cr 72.2 [52.3] S_B 87.6 [4.6] S_A 104.2[b] N 105.1[b] [8.2][c] I
A_2	$CH_2=CH-COO-C_6H_{12}O-$	$-OC_6H_{13}$	Cr 70.0 [42.6] S_B 76.8[d] [4.2] S_C 82.4[b] S_A 100.1 [0.8] N 118.2 [3.6] I
A_3	$H_{13}C_6O-$	$-OC_6H_{12}-OOC-CH=CH_2$	S_2 24.1 [5.2] S_1 55.0[b] S_B 86.9 [5.6] S_C 88.9 N 120 [3.1] I
B_1	$CH_2=CH-COO-C_{11}H_{22}O-$	$-OC_{11}H_{22}-OOC-CH=CH_2$	Cr_1 54.5[e] Cr_2 61.6[e] [24][f] S_B 98.8 S_A 103.1[e] [23.2][g] I
B_2	$CH_2=CH-COO-C_{11}H_{22}O-$	$-OC_6H_{13}$	S_B 45.6[h] [-26.2] Cr 67.3 [34.2] S_B 92.4 [4.9] S_A 112.2 N 116.2[e] [8.4][c] I
B_3	$H_{13}C_6O-$	$-OC_{11}H_{22}-OOC-CH=CH_2$	S_3 17.8 [0.8] S_2 30.3[h] [-44.6] Cr 58.2 [53] (34.7[b] S_1)[i] S_B 88.0 [6.8] S_C 92.7[b] N 112.9 [4.5] I

[a] Data measured at 10 °C/min on the second heating. [b] Data obtained by POM. [c] Peaks overlap. Enthalpy data of the S_A−N−I transition. [d] Transition observed as a shoulder of the peak. Temperature data of the onset. [e] Temperature corresponding to the maximum of the peak. [f] Peaks overlap. Enthalpy data of the Cr−Cr transition. [g] Peaks overlap. Enthalpy data of the S_B−S_A−I transition. [h] Cold crytallization. Temperature read at the maximum of the peak. [i] Monotropic phase S_B−S_1 observed on the cooling scan.

Chart 2. General Structure

Comp.	R_1	R_2	Phase Transitions (°C) [kJ/mol][a]
C_1	$CH_2=CH-COO-C_6H_{12}O-$	$-OC_6H_{12}-OOC-CH=CH_2$	Cr 49.8 [34.3] S_B 89.0 [4.4] S_A 107.1 [9.2] I
C_2	$CH_2=CH-COO-C_6H_{12}O-$	$-OC_6H_{13}$	S_1 18.9[b] [-12.1] Cr_1 56.4 Cr_2 62.0[c] [38.9][d] S_B 100.6 [3.5] S_A 124.0 [8.4] I
C_3	$H_{13}C_6O-$	$-OC_6H_{12}-OOC-CH=CH_2$	Cr 28.5 [20.9] S_B 103.1 [4.1] S_A 124.2 [9.9] I
D_1	$CH_2=CH-COO-C_{11}H_{22}O-$	$-OC_{11}H_{22}-OOC-CH=CH_2$	Cr 63.6 [54.2] S_B 93.8 [8.1] S_A 99.4 [12.3] I
D_2	$CH_2=CH-COO-C_{11}H_{22}O-$	$-OC_{11}H_{23}$	Cr 72.6 [55.2] S_B 104.6 [7.5] S_A 114.0 [13.1] I
D_3	$H_{23}C_{11}O-$	$-OC_{11}H_{22}-OOC-CH=CH_2$	Cr 72.0 [52.3] S_B 103.5 [7.9] S_A 113.5 [12.8] I

[a] Data measured at 10 °C/min on the second heating. [b] Cold crytallisation. Temperature read at the maximum of the peak. [c] Temperature corresponding to the maximum of the peak. [d] Peaks overlap. Enthalpy data of the Cr−Cr transition.

photopolymerisation of liquid crystalline diacrylates.[7] This technology has been applied in the preparation of numerous optical foils, e.g., patterned retarders,[8] broadband circular polarizers,[9] wide viewing angle films,[10] and cholesteric color filters.[11] The thin-film polarizers described are based on ordered liquid crystalline acrylate mixtures containing dichroic dyes.[12] The dichroic dye (guest)−liquid crystal (host) interaction gives rise to cooperative motion that serves to align the dye in the specified direction determined by the ordered arrangement of the liquid crystal molecules. It was shown that sufficiently high dye order parameters are observed in the smectic B (S_B) phase. The polarization performance of these guest−host polarizers is comparable to the polarization performance of traditional sheet polarizers. Several points need further investigation in the optimization of dichroic dye mixtures in order to obtain high performance guest−host polarizers. One of the main drawbacks observed previously is that the order within the dichroic mixture was partly lost upon photopolymerisation of the acrylate end groups in the S_B phase. It was then pointed out that steric reasons could originate this order disruption, and that the cross-linking degree and proximity of the acrylate groups from the rigid mesogenic core could account for it. These two factors are related with two particular structural aspects of the polymerizable molecules: the number of acrylate groups and the length of the flexible spacer, respectively. The only known liquid crystalline diacrylates that fulfill the properties for making these highly ordered networks are derived from cyclohexane carboxylic acid (Figure 1a).[6] These materials have a lower internal polarization because there is no electronic interaction between the ester group and the alkoxy derived spacer due to the cyclohexyl ring. This effect that leads to a more apolar mesogenic group probably causes the formation of the smectic phase instead of the nematic phase usually observed for the compounds derived from only aromatic rings.[13]

With these ideas in mind, we undertook the study of new liquid crystalline acrylates that fulfill these requirements and represent an alternative to achieve high-order parameters and an attempt to overcome the problem derived from lost of order upon polymerization. Because avoiding the formation of cyclohexane rings simplifies the synthetic procedures

(5) (a) Yip, W. C.; Kwok, H. S.; Kozenkov, V. M.; Chigrinov, V. G. *Displays* **2001**, *22*, 27. (b) Seiberle, H.; Benecke, C.; Bachels, T. *SID Digest* **2003**, 1162. (c) Roosendaal, S. J.; van der Zande, B. M. I.; Nieuwkerk, A. C.; Orenga, J. T. M.; Doornkamp, C.; Peeters, E.; Bruinink, J.; van Haaren, J. A. M. M.; Takahashi, S. *SID Dig. Tech. Pap.* **2003**, 78. (d) van der Zande, B. M. I.; Nieuwkerk, A. C.; van Deurzen, M.; Renders, C. A.; Peeters, E.; Roosendaal, S. J. *SID Dig. Tech. Pap.* **2003**, 194.
(6) Peeters, E.; Lub, J.; Steebakkers, J. A. M.; Broer, D. J. *Adv. Mater.* **2006**, *18*, 2412.
(7) (a) Broer, D. J. *Radiation Curing in Polymer Science and Technology. Polymerisation Mechanisms*; Fouassier, J. P., Rabek, J. F., Eds.; Elsevier: London, 1993; Vol.,Chapter 12, p 383. (b) Broer, D. J.; Boven, J.; Mol, G. N.; Challa, G. *Makromol. Chem.* **1989**, *190*, 2255.
(8) van der Zande, B. M. I.; Roosendaal, S. J.; Doornkamp, C.; Steenbakkers, J.; Lub, J. *Adv. Funct. Mater.* **2006**, *16*, 791.
(9) Broer, D. J.; Lub, J.; Mol, G. N. *Nature* **1995**, *378*, 467.
(10) van de Witte, P.; Tuijtelaars, J.; van Haaren, J. A. M. M.; Stallinga, S.; Lub, J. *Jpn. J. Appl. Phys., Part 1* **1999**, *38*, 748.
(11) (a) Lub, J.; van deWitte, P.; Doornkamp, C.; Vogels, J. P. A.; Wegh, R. T. *Adv. Mater.* **2003**, *15*, 1420. (b) van de Witte, P.; Brehmer, M.; Lub, J. *J. Mater. Chem.* **1999**, *9*, 2087.
(12) Cox, R. J. *Mol. Cryst. Liq. Cryst.* **1979**, *55*, 1. (b) Gray, G. W. *Chimica* **1980**, *34*, 47. (d) Gray, G. W. *Dyes Pigments* **1982**, *3*, 203. (c) Ivashchenko, A. V.; Rumyantsev, V. G. *Mol. Cryst. Liq. Cryst.* **1987**, *150*, 3−167.

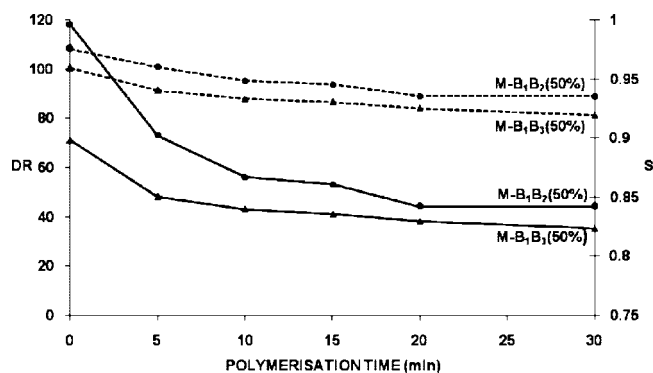(13) Lub, J.; van der Veen, J. H.; ten Hoeve, W. *Recueil Trav. Chim. Pays-Bas* **1996**, *115*, 321.

Figure 2. Dependence of the dichroic ratio *DR* (solid line) and order parameter (*S*) (dotted line) on the irradiation time for **M−B₁B₂ (50%)**, ●, and **M−B₁B₃(50%)**, ▲.

(Figure 1b), we designed monomers made only from aromatic rings of which one of the ester linking groups is replaced by an ethylene moiety (Figure 1c), thereby also decreasing the internal polarization in the mesogenic group. Moreover, the monomers prepared have different spacer lengths and different numbers and position of acrylate groups so that steric problems responsible for order disruption within the resulting network can be solved. The general target structure is represented in Charts 1 and 2. The compounds prepared are divided into four series. The compounds within each series share identical core structure and spacer length, and they differ only in the number or position of the acrylate groups.

The first part of this work deals with the preparation and mesomorphic characterization of the materials, polymerizable monomers as well as mixtures with dichroic dye. This aspect was important for the selection of the most appropriate liquid crystalline acrylates and dichroic mixtures to form the oriented network. This selection was based on the following requirements: The polymerizable monomers must possess a highly ordered smectic or soft crystalline phase; these highly ordered phases should preferably be stable at room temperature for at least 30 min to avoid crystallization during the alignment and photopolymerisation processes; the polymerizable monomer preferably exhibit a nematic phase that favors alignment of the material and the formation of a monodomain within the cell before cooling to the highly ordered phase.

The second part of this work is devoted to the study of the order induced within the polymerizable dichroic mixtures as well as the order achieved after in situ polymerization of uniaxially orientated cells.

Further, the dependence of the order on the temperature before and after photopolymerisation (e.g., the thermal stability of the networks) was investigated.

Experimental Section

The synthetic procedures for the formation of the compounds can be found in the Supporting Information.

¹H and ¹³C NMR spectra were recorded on a VARIAN Unity-300, BRUKER ARX-300, or BRUKER AV-400 spectrophotometers (with frequency of 300 or 400 MHz for 1H, 75 or 100 MHz for ¹³C). Deuterated solvents as CDCl₃, acetone-d₆, or DMSO-d₆ were used in function of the compound solubility.

The ¹H and ¹³C NMR data were fully consistent with the required chemical structures and confirmed the purity of the final compounds. Elemental analysis of C, H, N, and S was carried out in an elemental analyzer LECO CHNS-932. Infrared (IR) spectra were collected in a NICOLET Avatar 380 spectrophotometer. The samples were prepared according to the type of compound: KBr pellets or nujol suspension for solid compounds and neat preparation for liquids. Mass spectrometry of the final compounds was carried out by the ionization method of FAB+ and 3-nitrobenzyl alcohol (NBA), in a VG AutoSpec EBE spectrometer.

Study of the Mesomorphic Behavior. All the monomers and the dichroic mixtures were studied by polarized optical microscopy (POM) at variable temperature, differential scanning calorimetry (DSC) and X-ray diffraction (XRD) at variable temperature. To avoid thermal polymerization, the radical inhibitor (2,6-di-*tert*-butyl-4-methylphenol) was added in an amount of 200 ppm for each monomer. In addition, the optical microscopic studies were carried out using a Lambda Research Optic Inc. filter, which eliminated light with a $\lambda < 400$ nm, thus avoiding photoinduced polymerization. Working laboratory conditions were also adapted with a suitable light source to avoid the photopolymerisation of samples.

Polarized optical microscopy was carried out with an OLYMPUS BH-2 microscopy with crossed polarizers and a heating hotstage LINKAM THMS600 controlled by a LINKAM TMS91 temperature controller. A LINKAM CS196 cooler system with liquid nitrogen was connected to the microscope to the study the mesomorphic behavior of the samples at temperatures below room temperature. The microphotographs were recorded with an Olympus digital camera, DP-12, connected to the microscope and controlled by DP-Soft software. Differential scanning calorimetry (DSC) was carried out with a TA Instruments DSC-MDSC 2910 equipment making use of powder samples (aprox 2−5 mg) in sealed aluminum pans. Temperature data were obtained in the onset for sharp peaks and the maximum of the peak for broad peaks. All the DSC studies were carried out with a scanning rate of 10 °C/min on both heating and cooling processes from temperatures below room temperature to 20 °C above the temperature to the isotropic transition temperature observed by POM. X-ray diffraction was carried out in a PINHOLE (Antón-Paar) camera that makes use of a collimated Ni-filtered Cu Kα beam. Samples were introduced in Lindemann glass capillaries (0.9 mm diameter) and heated by means of a variable temperature oven. Diffratograms were registered in flat photographic films situated to a variable distance from the sample. The capillary axis and the film were perpendicularly situated to the X-ray beam. The theoretical molecular length was calculated using Dreiding models assuming the all-trans conformation of the alkoxy chains.

Preparation of the Dichroic Mixtures. The exact amount of the liquid crystal host components was weighted in an amber vial and dissolved in a low boiling solvent as dichloromethane. The corresponding volumes of previously prepared solutions of dichroic dye (2 mg/mL), photoinitiator (1 g/mL), and inhibitor (0.1 g/mL) in dichloromethane were added. To ensure homogeneous mixing of all the components and prevent crystallization of the mixture, the solvent was evaporated at a temperature above the melting point of the liquid crystalline acrylate.

Thin Films of Dichroic Mixtures. Commercial Linkam cells of 5 μm gap with inner surfaces covered by a thin layer of polyimide uniaxially rubbed and antiparallel alignment were used for the preparation of the macroscopically orientated films of the dichroic mixtures. Cells were filled by capillary action at elevated temperatures, preferably 10−20 °C above the clearing temperature of the liquid crystalline material, to ensure a complete miscibility of the components of the mixture. However, the temperature cannot exceed

Scheme 1. Synthesis of 4-(4-(6-(Acryloyloxy)hexyloxy)phenethyl)phenyl 4-(6-(Acryloyloxy)hexyloxy)benzoate (A₁)
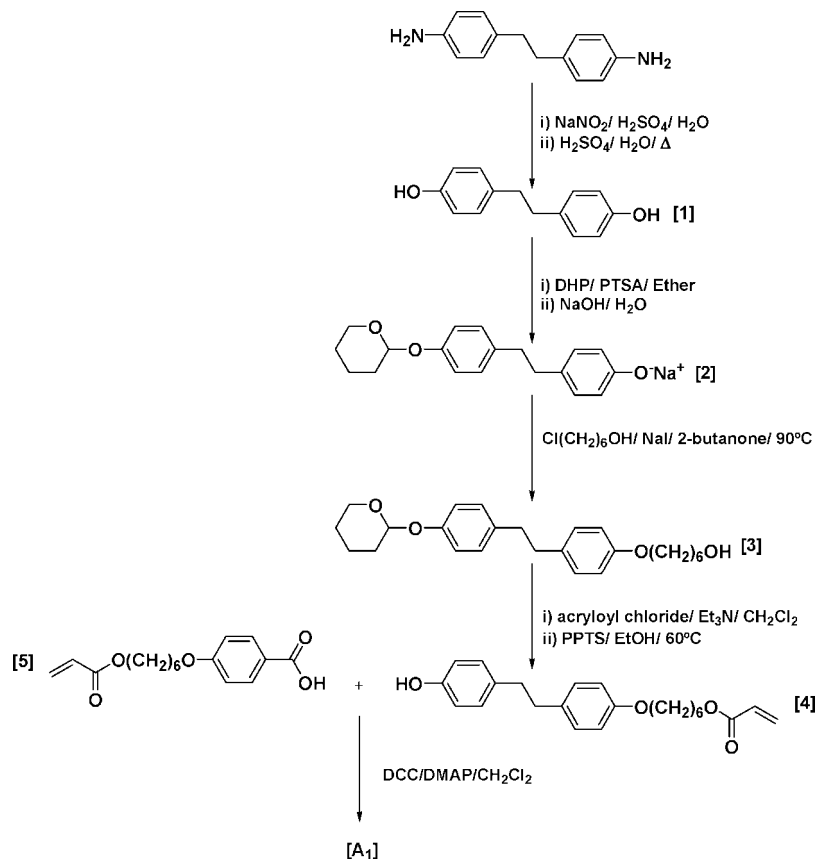
130 °C because unwanted thermal polymerization reactions could occur. The presence of the polyimide layers induces homogeneous (planar) alignment of the liquid crystal molecules in a single monodomain along the rubbing direction.

Photopolymerization. Photopolymerization was carried out using a UV-Philips PL-S 9W/10 lamp whith maximum emission at 365 nm. To set the conditions for the photopolymerization experiments, the dichroic ratio (*DR*) and order parameter (*S*) of two of the mixtures was studied versus polymerization time (Figure 2). It can be seen that stabilization of both magnitudes occurs at exposure times longer than 15 min. Consequently, the exposure time was set to 20 min for all the experiments with the lamp at a distance of 10 cm from the sample.

Measurement of the Order Parameter. Measurements were performed in a double beam Unicam UV/vis Spectrometer UV4 modified to incorporate a Mettler FP82 hot-stage with a Mettler FP80 controller. The UV spectrometer was also modified by incorporating a rotating polarizer. The correct alignment of all the elements was checked by performing measurements at different angles to ensure that the maximum absorption was registered. During the study, the cell was heated above the clearing point, and then was cooled gradually at a rate of 5 °C/min. Polarized UV/vis absorption, parallel and perpendicular to the liquid crystal director, was recorded every 10 °C. A cell filled with a mixture that contains the host liquid crystal, the inhibitor, and the initiator was used as reference. The reference cell compensated the losses due to absorption, scattering, and reflection from the cell walls and host molecules. Because the highest dichroic ratio was determined at room temperature, the reference spectra was determined only at room temperature. For all the mixtures, at least a minimum of two cells were prepared and measured in order to compensate possible experimental errors or defects in a particular cell. Dichroic ratios given are the averaged values obtained from the *DR* calculated

between 470 and 570 nm, where the maximum absorbance is located.

Results and Discussion

Synthesis of the Monomers. The liquid crystalline monomers were prepared by convergent syntheses in which the final step was the esterification of a carboxylic acid and the corresponding phenol. As an example, the syntheses of compounds **A₁** and **C₁** are outlined in Schemes 1 and 2, respectively. The synthetic pathways for the formation of compounds **A₂**, **A₃**, **B₁**−**B₃** are similar to that of **A₁**, and those for the formation of compounds **C₂**, **C₃**, **D₁**−**D₃** are similar to that of **C₁**. The synthetic strategies were planned in a way that intermediate compounds could be used as building blocks for more than one end product.

The synthetic route to prepare compound **A₁** (Scheme 1) starts with the preparation of 1,2-bis(4-hydroxyphenyl)ethane (**1**) from commercial 1,2-bis(4-aminophenyl)ethane by preparation of the diazonium salt and subsequent hydrolysis with water in acidic media. The monoprotected tetrahydropyranyl-ether phenoxide **2** was obtained in conditions similar to that described in the literature for hydroquinone or 4,4′-hydroxy-biphenyl derivatives.[14] The poor solubility of the sodium salt of the monoprotected derivative (**2**) in basic aqueous media, and in acetone, provided an easy way for isolating the compound from the starting material (**1**) and the diprotected compound, simply by extraction of the solid sodium salt.

(14) Hikmet, R. A. M.; Lub, J.; Tol, J. W. *Macromolecules* **1995**, *28*, 3313.

Scheme 2. Synthesis of 4-(6-(Acryloyloxy)hexyloxy)phenyl 4-(4-(6-(Acryloyloxy)hexyloxy)phenethyl)benzoate (C₁)
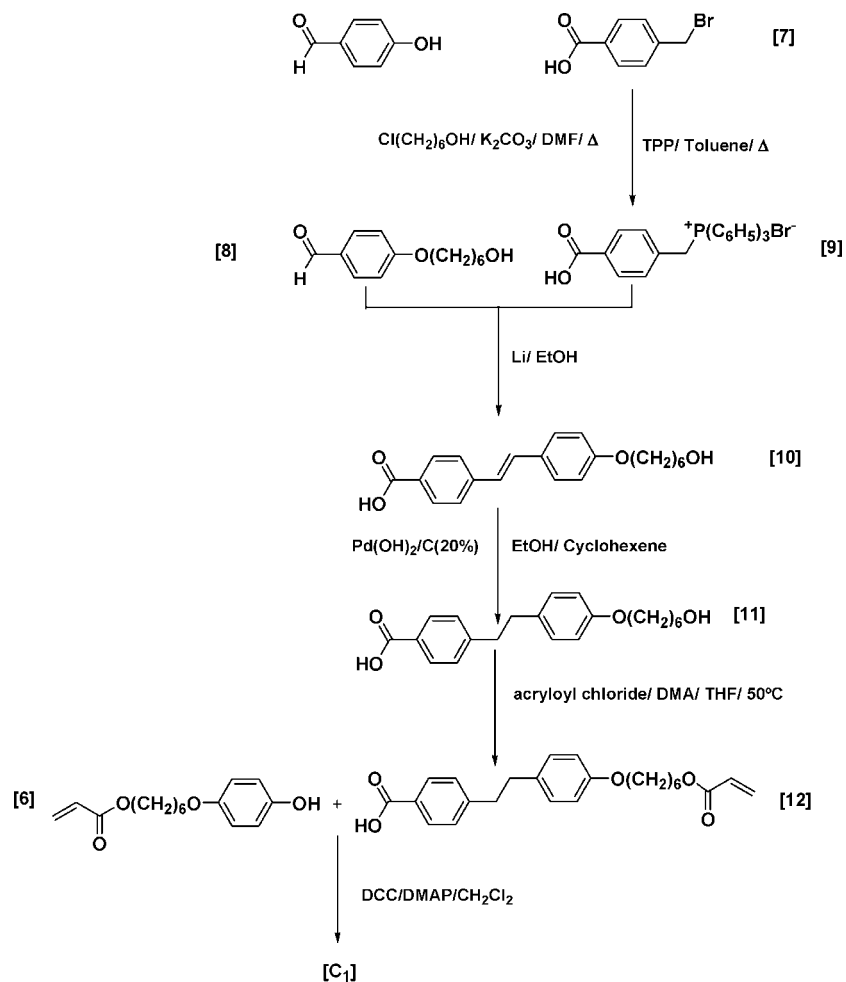
The hexamethylene spacer present in phenol **4** was introduced by etherification of phenoxide **2** with 6-chlorohexanol in butanone. In the subsequent step, the acrylate group was introduced by condensation of acryloyl chloride with the terminal hydroxyl group in the presence of triethylamine. The final removal of the tetrahydropyranyl ether group with pyridinium *p*-toluenesulfonate in ethanol afforded the corresponding phenol **4**. The final product **A₁** was formed after esterification between phenolic derivative **4** and acrylate-derived acid **5**. The latter acid was prepared according the literature.[15]

Scheme 2 shows the synthetic pathway to prepare acid derivative **12** that was esterified with phenolic derivative **6** to form compound **C₁**. Compound **6** was prepared according the literature.[16] The stilbene-derived acid **10** was synthesized by a Wittig reaction between triphenylphosphonium bromide **9**, made from bromide **7**, and aldehyde **8**, which was synthesized by etherification of 4-hydroxybenzaldehyde following standard Williamson conditions. The Wittig reaction was performed in ethanolic media, using 2 equiv of lithium ethanolate followed by acidification. During the course of the reaction, both *E* and *Z* isomers of **10** were formed. The *E* isomer precipitates and was easily obtained by filtration after acidification, whereas the *Z* isomer remained in solution. The *E* isomer was used in the hydrogenation with Pd(OH)₂ on carbon in ethanol and cyclohexene to form carboxylic acid **11**. Finally, acrylate-derived acid **12** was prepared by reacting acryloyl chloride with **11** in dry tetrahydrofuran and *N,N*-dimethylaniline (DMA) as base.

Liquid Crystalline Properties of the Monomers. All the monomers were studied by polarized optical microscopy (POM) at variable temperatures, differential scanning calorimetry (DSC), and X-ray diffraction (XRD) at variable temperatures. Phase transitions were determined from DSC and POM, whereas phase identification was first made by observing the corresponding textures by POM[17] and further confirmed by XRD diffraction. The phase transition temperatures and enthalpies of all compounds are gathered in Charts 1 and 2.

The nematic phase was usually identified by its fluid *schlieren* texture. Additionally, compound **B₃** showed a homeotropic texture for the nematic phase at lower temperatures.

(15) Broer, D. J.; Boven, J.; Mol, G. N.; Challa, G. *Makromol. Chem.* **1989**, *190*, 2255.

(16) van der Zande, B. M. I.; Steenbakkers, J.; Lub, J.; Leewis, C. M.; Broer, D. J. *J. Appl. Phys.* **2005**, *97*, 123519/1.

(17) (a) Gray, G. W.; Goodby, J. W. *Smectic Liquid Crystals: Textures and Structures*; Leonard Hill: Glasgow, Scotland, 1984. (b) Collings, P. J.; Hird, M. *Introduction to Liquid Crystals—Chemistry and Physics*; Gray, G. W., Goodby, J. W., Fukuda, A., Eds.; Taylor & Francis: London, 2001. (c) Dierking, I. *Textures of Liquid Crystals*; Wiley-VCH: Weinheim, Germany, 2003.
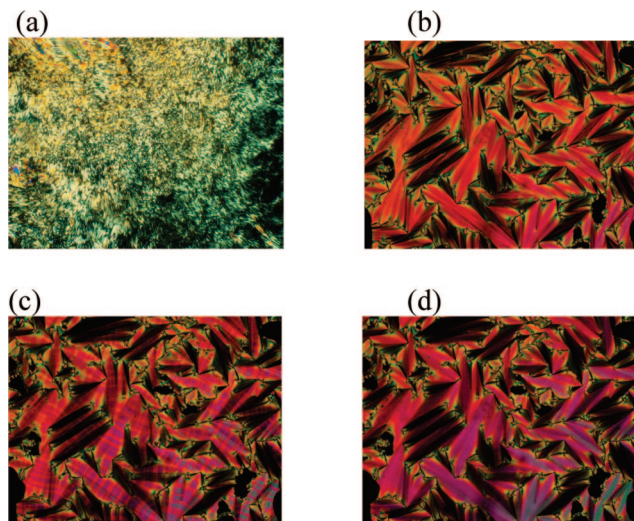
Figure 3. (a) Texture of the S_B phase after mechanical shearing of the homeotropic texture at 64 °C for compound A_2 during cooling. Sequence of textures observed for compound A_1 during the cooling process: (b) fan-shaped texture of the S_A phase at 90 °C; (c) transitions bars observed in the S_A−S_B transition at 88.4 °C; and (d) fan-shaped texture of the S_B phase at 88 °C.

The natural texture observed of the optically uniaxial S_A phase, on cooling from the isotropic liquid or the nematic phase, was usually the homeotropic texture. Some compounds showed focal-conic or fan-shaped textured areas (see Figure 3b) in addition to the homeotropic areas. The S_B phase exhibited the paramorphotic focal-conic and homeotropic textures when formed on cooling the S_A phase. For this reason, the S_A−S_B transition was often missed by optical microscopy. In the homeotropic texture, no differences between both phases were detected unless mechanical treatment of the sample was carried out. Pressing the sample when it is in the S_A phase, the sample remains black and fluid. After pressing while in the S_B phase, a different texture, not completely black, was detected (see Figure 3a). In the fan-shaped texture, both phases can be distinguished because very smooth cones are seen in the S_B phase, with a clear, blemish-free back and no lines running from the fan apexes (see Figure 3d). Diacrylate A_1 showed transition bars on cooling from the S_A to the S_B phase (Figure 3c), which are indicative of a CrB phase.[17a,b,18] However, since these observations were not conclusive, and X-ray measurements did not allow confirmation of the CrB phase, the notation S_B appears for the mesomorphic behavior of A_1.

Compounds A_2 and A_3 showed an additional tilted S_C phase on cooling from the orthogonal S_A or the N phases, respectively. The *schlieren* texture of the S_C phase was generated from the homeotropic texture of the upper S_A phase or the *schlieren* texture of the nematic mesophase. Monoacrylates A_3, B_3, and C_2 showed rich smectic polymorphism. Their DSC thermograms showed several peaks, which correspond to the formation of unidentified smectic mesophases, labeled as S_1, S_2, and S_3. The S_1 mesophase (A_3 and B_3) was observed by optical microscopy in both compounds. Its XRD diffraction pattern, taken at 40 °C in A_3, indicated

(18) (a) Goodby, J. W.; Pindak, R. *Mol. Cryst. Liq. Cryst.* **1981**, *75*, 233. (b) Lam, J. W. Y.; Dong, Y.; Check, K. K. L.; Luo, J.; Xie, Z.; Kwok, H. S.; Mo, Z.; Tang, B. Z. *Macromolecules* **2002**, *35*, 1229.

Table 1. X-ray Diffraction Data of Series A, B, C, and D Compounds[a]

compd	D (Å)	d (Å)	T (°C)	mesophase
A₁	46	42	90	S_A
		44	75	S_B
A₂	41	39	86	S_A
		40	64.6	S_B
A₃	41	39	60	S_B
		36	40	S_1
B₁	59	56	77.7	S_B
B₂	47	44	102.9	S_A
		45.7	35.2	S_B
B₃	47	45.7	35	S_B
C₁	46	40.6	91.9	S_A
		42.3	76.4	S_B
C₂	41	37.5	110	S_A
		39	50	S_B
C₃	41	37.5	110	S_A
		39	50	S_B
D₁	59	56	70	S_B
D₂	54	49.3	109	S_A
		51	79.7	S_B
D₃	54	47.4	111	S_A
		51.4	79.8	S_B

[a] T (°C), temperature of the X-ray experiment; D (Å), molecular lengths calculated by means of Dreiding models; d (Å), Lamellar spacing determined from the reflections observed at low angles in the diffractograms.
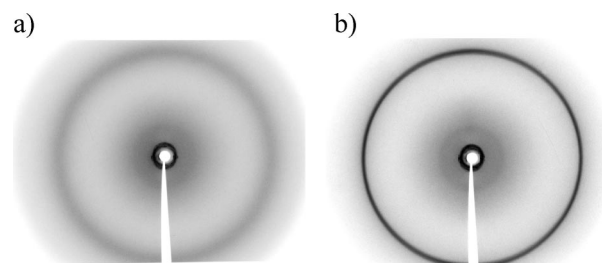

Figure 4. (a) X-ray diffraction pattern at 90 °C for monoacrylate A_1 in the S_A phase. (b) X-ray diffraction pattern at 75 °C for monoacrylate A_1 in the S_B phase.

that it was a tilted smectic phase as it showed a decrease in the lamellar spacing (respect to the upper S_B phase) associated with tilting of the molecules. The lower temperature mesophases S_2 and S_3 could not be identified by the optical textures observed by microscope.

XRD provided the structural parameters of the S_A and the S_B mesophases, which are gathered in Table 1.

Reflections observed at wide angles also provided important information related to the order of the molecules within the layers. Figure 4a shows a typical XRD pattern of a S_A phase, and it corresponds to monomer A_1. The diffuse nature of the outer ring was characteristic of the liquidlike arrangement of molecules in the layers. The XRD pattern of the S_B phase of compound A_1 (Figure 4b) showed a relatively sharp outer-ring while the inner ring was well defined and sharp. The lamellar spacing calculated for this phase fitted better with the theoretical values (D) than for the S_A phase because the alkylene spacer groups are in a more extended conformation in this ordered mesophase.

In conclusion, the collected data from the polarized optical microscopy, X-ray diffraction, and differential scanning calorimetry show that all compounds exhibit the highly ordered S_B phase. However the data also show that all compounds in series **C** and **D** lack a nematic phase that is
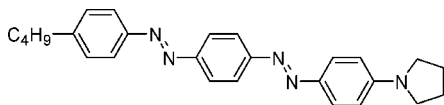
Figure 5. Chemical structure of the G205 azo-dye.

needed for the monolithic alignment of the monomers. Apparently, the inverse orientation of the ester linking group in series **C** and **D** with respect to series **A** and **B** induces smectic-type mesomorphism. Compounds of series **A** do show a nematic phase, whereas in series **B** only the monoacrylate compounds **B₂** and **B₃** show a nematic phase before clearing. The substitution of the hexyloxy spacers of **A₁** by undecyloxy spacers of **B₁** causes a decrease of the mesomorphic interval and disappearance of the nematic phase.

Dichroic Liquid Crystal Mixtures. On the basis of the results above, compounds of series **A** and **B** were selected for the preparation of the polymerizable liquid crystal mixtures. For the sake of simplicity, liquid crystalline matrices were prepared by mixing only compounds belonging to the same series. A total of 17 dichroic liquid crystal mixtures were prepared based on pure monomers as well as blends of a diacrylate and a monoacrylate in different weight proportions (25:75, 50:50, and 75:25). Each liquid crystal matrix was mixed with 1 wt/wt% photoinitiator, 2,2-dimethoxy-2-phenylaceophenone (Irgarcure 651, Ciba-Geigy), 2 wt/wt% of the dichroic dye G205 (Hayashibara Biochemical Laboratories, Inc.), and 0.1 wt/wt% of *p*-methoxyphenol as radical inhibitor in order to prevent unwanted thermal polymerization during processing. The azo dye G205 (Figure 5) was chosen from previous studies, which demonstrated its high dichroic ratio in various liquid crystal matrices. The different mixtures were compared on their mesomorphic behavior and degree of order and were used to study the influence of the cross-link density on the optical properties and stability of the networks.

First, the phase behavior of the mixtures was studied. Basically, the mesomorphic behavior of a dichroic liquid crystal mixture is governed by that of the liquid crystal host. Nevertheless, the addition of the dye effects the mesophase interval depending on the structural compatibility between the matrix and the dye.[19,20] In addition to the transition temperatures of the mixtures, it was important to determine the homogeneity of the samples during the cooling process using optical microscopy and DSC. The phase sequence and the phase transition temperatures of all the mixtures prepared are gathered in Table 2. Series **A** mixtures are characterized by quite short nematic and S_A phase intervals, and broad S_B phase intervals near room temperature. The S_C phase observed for monomer **A₂** could not be detected in its dichroic mixture **M−A₂**, or in any of the mixtures with

diacrylate **A₁**. The dichroic mixture with only diacrylate **B₁** was not prepared because this monomer did not exhibit the nematic phase. Moreover, the nematic phase was not observed for any of the blends that included a high percentage of diacrylate **B₁** (75%) in their formulation. All the blends in this series exhibited the S_A phase, except **M−B₃**, and broad S_B phase intervals. In addition, **M−B₃** and **M−B₁B₃(25%)** exhibited the S_C phase within a short temperature interval. It is also important to emphasize that these blends could be maintained in their supercooled liquid crystal phase at room temperature for a long time before crystallization took place.

Subsequently, the order parameter was studied for the different mixtures by aligning the mixtures inside liquid crystal cells with 5 μm cell gap and antiparallel alignment. Upon alignment of a liquid crystalline host by surface forces, the dye molecules are aligned simultaneously by guest−host interactions along the director of the host liquid crystals, resulting in dichroic absorption of the mixture. Dichroic ratios in absorption were determined from polarized UV/vis spectroscopy before and after photopolymerization of the dichroic liquid crystal mixtures.

The long-range orientational order, which is a characteristic feature of liquid crystal materials, can be described by the order parameter, S.[21] Under the assumption that the transition dipole moment for the G-205 dye molecules is located along the long axes of the dye molecule the average order parameter for dye molecules, S_{dye}, can be calculated experimentally from the dichroic ratio of the dye DR (eq 1)[20]

$$S = \frac{A_{\parallel} - A_{\perp}}{A_{\parallel} + 2A_{\perp}} = \frac{DR - 1}{DR + 2} \tag{1}$$

where the dichroic ratio ($DR = A_{\parallel}/A_{\perp}$) is determined from the absorption of polarized light by the dye molecules in the parallel ($A_{\parallel}$) and perpendicular ($A_{\perp}$) liquid crystal alignment direction.

Figure 6 shows the polarized UV/vis spectra of mixture **M−A₁A₂ (75%)** under 0 and 90° with respect to the alignment direction, recorded at different temperatures.

For the isotropic liquid at 120 °C, $DR = 1$ indicated the total absence of order (see Figure 6a). The polarized UV/vis spectra recorded in the nematic phase (Figure 6b) show the anisotropic order induced in the dye molecules by the liquid crystal matrix due to guest−host interactions, which depend on the temperature and on the nature of the mesophase. Figure 7 represents the variation of DR and S with temperature corresponding to the mixture **M−A₁A₂(75%)**. At 110 °C, the observed dichroic ratio is 5 and corresponds to an order parameter $S = 0.57$, which is in a agreement with the order parameter measured for nematic phases of similar reactive liquid crystals.[22] When the sample was cooled further, other mesophases with a

(19) (a) Diot, P.; Foitzik, J. K.; Haase, W. *Rev. Phys. Appl.* **1985**, *20*, 121. (b) Kozielski, M.; Bauman, D.; Drozdowski, M.; Salomon, Z. *Mol. Cryst. Liq. Cryst.* **1987**, *142*, 1. (c) Haase, W.; Trinquet, O.; Quotschalla, U.; Foitzik, J. K. *Mol. Cryst. Liq. Cryst.* **1987**, *15*, 148. (e) Bauman, D. *Mol. Cryst. Liq. Cryst.* **1988**, *159*, 197. (f) Bauman, D. *Mol. Cryst. Liq. Cryst.* **1989**, *41*, 172. (g) Bauman, D.; Martyński, T.; Mykowska, E. *Liq. Cryst.* **1995**, *18*, 607.
(20) Ivashchenko, A. V.; Petrova, O. S.; Titov, V. V. *Mol. Cryst. Liq. Cryst.* **1984**, *108*, 51.

(21) Collings, P. J.; Hird, M. *Introduction to Liquid Crystals*; Taylor & Francis: London, 1998.
(22) Goodby, J. W. *Handbook of Liquid Crystals*; Demus, D., Goodby, J. W., Gray, G. W., Spiess, H.-W., Vill, V., Eds.; Wiley-VCH: Weinheim, Germany, 1998; Vol. 2A, Chapter I.
(23) The average dichroic ratio and order parameter values calculated at the different temperatures for the dichroic mixtures of Series **A**, **B** are included in the Supporting Information.

Table 2. Mesomorphic Properties of the Dichroic Mixtures

mixture[a]	transition temperatures (°C)[b]	$\Delta T \, S_B$
M−A₁	I 104[c] N 100.9[d] S_A 83.5 S_B −2 Cr	85.5
M−A₁A₂(75%)	I 108 N 101.2[d] S_A 79.7 S_B −3 Cr	83
M−A₁A₂(50%)	I 111 N 99[d] S_A 75 S_B −3 Cr	78
M−A₁A₂(25%)	I 116 N 101[d] S_A 74 S_B 0.4 S₁[e]	73.6
M−A₂	I 119.7 N 99.7 S_A 69.9 S_B	>70
M−A₁A₃(75%)	I 108.5 N 101.5[d] S_A 81.7 S_B 0.21 Cr	81.5
M−A₁A₃(50%)	I 111 N 99.8 S_A 80.2 S_B 3 S₁[e]	77.2
M−A₁A₃(25%)	I 115 N 96 S_A 81.3 S_B 9.3 S₁[e]	72
M−A₃	I 120 N 83 S_C 80.6 S_B 47[c] S₁[e] 13.7 Cr	33.6
M−B₁B₂(75%)	I 106.3 S_A 92.8 S_B 9.5 Cr	83
M−B₁B₂(50%)	I 109.6 N 107.7[f] S_A 90 S_B	>90
M−B₁B₂(25%)	I 111.5 N 107.9[d] S_A 88.8 S_B	>89
M−B₂	I 116.6 N 111.4[d] S_A 87.6 S_B	>88
M−B₁B₃(75%)	I 104.3 S_A 90.7 S_B 13.9 Cr	77
M−B₁B₃(50%)	I 106[c] N 102.8[d] S_A 88.2 S_B 18[f] S₁[e] 8.9 S₂[e] 7.85 Cr	70
M−B₁B₃(25%)	I 109 N 101[d] S_A 86.2 S_C 84.8 S_B 16[f] S₁[e] 8.9 S₂[e] 2.6 S₃[e]	70
M−B₃	I 114.2 N 93[f] S_C 83.9 S_B 35[f] S₁[e] 14.5 S₂[e] 5.9 S₃[e]	49

[a] Blends are denoted by letter M followed by the code of the different reactive monomers included in the mixture formulation. Percentage indicated between brackets corresponds to the percentage of diacrylate included in the mixture. [b] Data measured at 10 °C/min on the third cooling scan. [c] Transition detected as a shoulder. [d] Data corresponds to the value of the peak maximum. [e] Unidentified phases. [f] POM data.
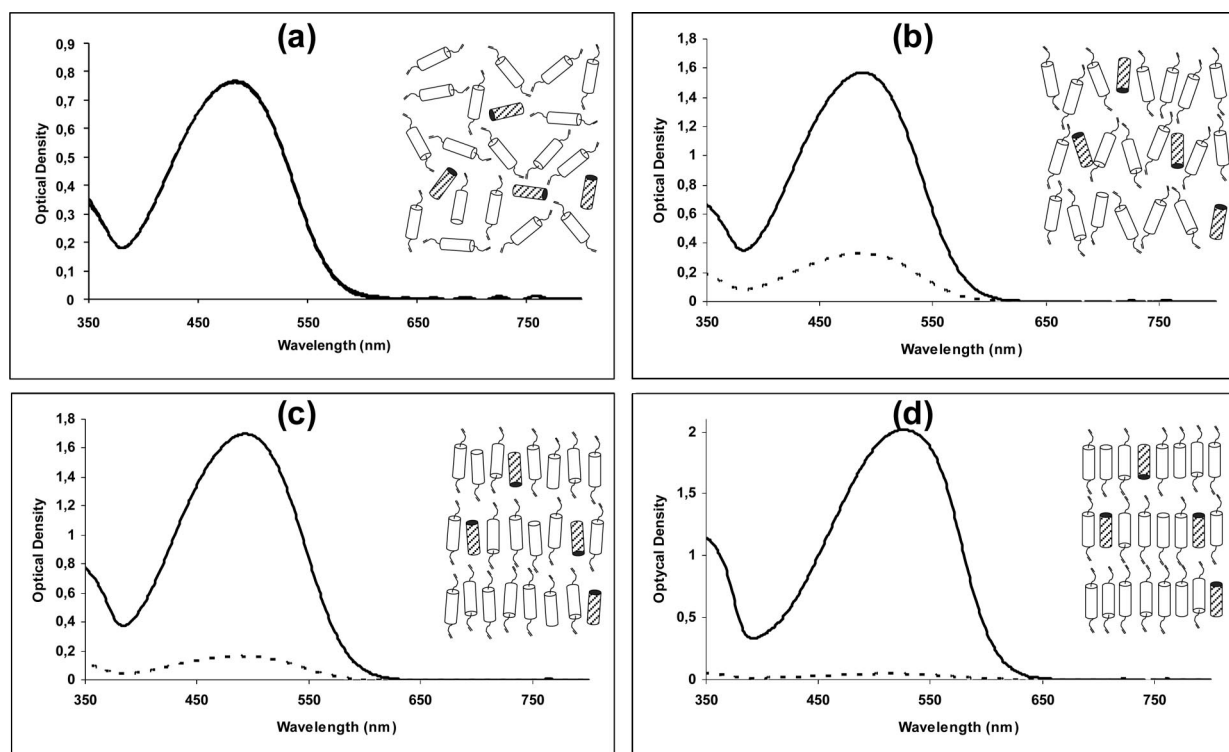
Figure 6. Polarized UV/vis spectra of **M−A₁A₂(75%)** (a) in the isotropic liquid $DR = 1$ and $S = 0$; (b) in the Nematic phase, $DR = 5$, $S = 0.7$; (c) in the S_A phase at 100 °C, $DR = 12$, $S = 0.79$; (d) in the S_B phase at 30 °C, $DR = 44$, $S = 0.93$. The solid line represents absorbance in the parallel direction, dotted line represents absorbance in the perpendicular direction. White cylinders represent the reactive mesogen, gray cylinders represent dichroic dye molecules.

higher order than the nematic phase appeared. Figure 6c shows the polarized UV/vis spectra of **M−A₁A₂(75%)** in the S_A phase. The difference between the UV/vis curves in the perpendicular and parallel direction to the director of the cell increased strongly, which occurs parallel to the appearance of lamellar arrangement. This was confirmed by an increase in the calculated dichroic ratio ($DR = 12$) and order parameter ($S = 0.79$). A significant decrease in the maximum absorbance in the perpendicular direction was clearly observed when spectra are recorded in the S_B phase, Figure 6d, which gives rise to an increase of the dichroic ratio ($DR = 44$) and order parameter ($S = 0.93$). This behavior of DR

and S against temperature was observed for all the mixtures,[23] which showed their highest values in the S_B mesophase, as expected. Table 3 gathers DR and S data measured at room temperature for all the mixtures studied.[24]

The dichroic ratio and order parameter values obtained for the S_B phase at room temperature ($DR = 50$ to >90, S

(24) Several attempts were made to align mixtures **M−B₁B₂(75%)** and **M−B₁B₃(75%)** cooling from the I−S_A transition temperature at low cooling rates, i.e., 0.5−1 °C/min. Even though the cells looked transparent, they showed multiple defects under the microscope, which confirmed that alignment did not occur in a single monodomain.

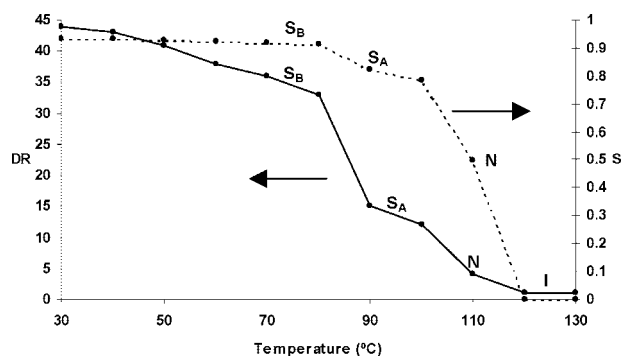(25) Broer, D. J.; Hikmet, R. A. M.; Challa, G. *Makromol.Chem.* **1989**, *190*, 3201.

Figure 7. *DR* and *S* vs temperature for **M−A₁A₂(75%)**.

Table 3. *DR*ₘᵢₓ, Average Dichroic Ratio Values for the Mixtures Calculated at 30°C; *S*ₘᵢₓ, Average Order Parameter Values Calculated for the Mixtures at 30°C; *DR*ₚₒₗ, Average Dichroic Ratio Values of the Polymer at Room Temperature; and *S*ₚₒₗ, Average Order Parameter Values of the Polymer at Room Temperature

mixture	$DR_{mix}{}^a$	$S_{mix}{}^a$	$DR_{pol}{}^a$	$S_{pol}{}^a$
M−A₁[b]	45	0.94	30	0.91
M−A₂[b]	46	0.94	41	0.93
M−A₃[c]	43	0.93	36	0.92
M−A₁A₂(75%)[b]	44	0.93	38	0.93
M−A₁A₂(50%)[b]	41	0.93	35	0.92
M−A₁A₂(25%)[b]	43	0.93	35	0.92
M−A₁A₃(75%)[b]	38	0.93	34	0.92
M−A₁A₃(50%)[b]	40	0.93	29	0.90
M−A₁A₃(25%)[b]	42	0.93	38	0.93
M−B₂[b]	>90	0.98	48	0.94
M−B₃[c]	61	0.95	52	0.94
M−B₁B₂(50%)[b]	>90	0.97	52	0.94
M−B₁B₂(25%)[b]	>90	0.98	50	0.94
M−B₁B₃(50%)[b]	60	0.95	39	0.93
M−B₁B₃(25%)[b]	52	0.94	37	0.92

[a] Averaged values calculated between 470 and 570 nm, where the maximum absorbance is located. For all the mixtures, data correspond to the average values calculated for at least a minimum of two cells. [b] DR_{mix} and S_{mix} values calculated in the S_B phase. Sample polymerized in the S_B phase. [c] DR_{mix} and S_{mix} values calculated in the unidentified S₁ phase. Sample polymerized in the S₁ phase.

= 0.94−0.98) for the mixtures within Series **B** were clearly the highest ones measured for all mixtures examined in this study. The average *DR* and *S* values calculated for blends that include monoacrylate **B₂** in their formulation are higher than those which have monoacrylate **B₃**. As the percentage of **B₂** increases in the formulation, the *DR* measured increased, measuring the highest value for the pure monoacrylate mixture. It is remarkable that the monoacrylates **A₂** and **B₂**, in which the acrylate group is in the benzoate moiety of the molecule, exhibited higher order degree than monoacrylates with the acrylate group in the opposite position, **A₃** and **B₃**.

Upon photopolymerization of orientated monomers in the S_B phase all samples decrease their order (Figure 8), in contrast to what has been observed for the nematic phase.[25] After ruling out the possibility of the cis−trans isomerization of the azo dye being responsible for this,[6] it was pointed out that the reason would mainly lie in steric factors.

It is thought that the reduction in dichroic ratio can be caused by some disruption of the order of the central mesogenic units in the smectic B phase as a result of the formation of a highly cross-linked polymer network. Because of the steric restrictions imposed by cross-linking, the free volume decreases causing a loss of orientation of the molecules with respect to the starting
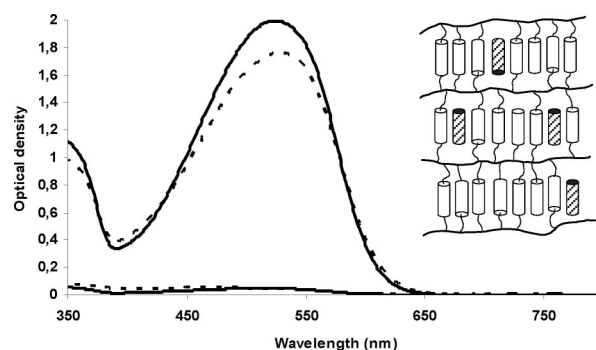

Figure 8. Polarized UV/vis spectra of **M−A₁A₂(75%)** in the S_B phase before polymerization (solid line) at 30 °C, *DR* = 44, *S* = 0.93. and after polymerization (dotted line) at RT, *DR* = 38, *S* = 0.93.
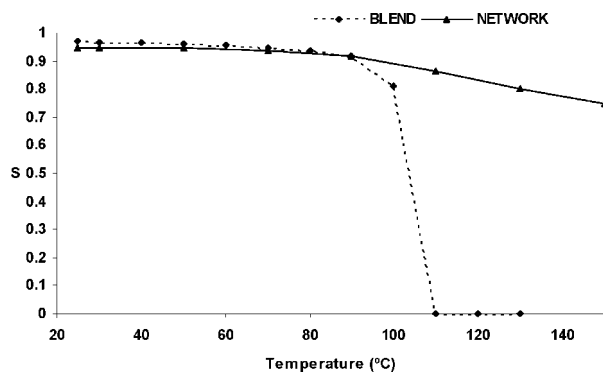

Figure 9. Thermal stability of the polymeric film prepared from **M−B₁B₂(50%)** compared with the thermal behavior of the dichroic mixture **M−B₁B₂(50%)**.

monomers. Consequently, dye molecules must accommodate within a less-ordered state as they must adapt to the new free volume imposed by the network. The influence of the cross-link density on the loss of order during photopolymerisation was studied by partially or completely replacing diacrylate monomers by monoacrylates, which produces in the extreme side a noncross-linked linear polymer. Within the series **M−A₁**, **M−A₁A₂(75%)**, **M−A₁A₂(50%)**, **M−A₁A₂(25%)**, **M−A₂**, the diacrylate content is gradually decreased going from 100% for the **M−A₁** mixture to 0% for the **M−A₂** mixture. The polarized UV/vis measurements before and after polymerization show that there is a considerable decrease in the dichroic ratio during polymerization for the pure diacrylate mixture **M−A₁** (34% decrease), Mixing in 25% of monoacrylate **A₂** has a significant influence on the decrease in order during polymerization. For **M−A₁A₂(75%)** the decrease in dichroic ratio during polymerization only amounted to 14%. Further increasing the monoacrylate content does not affect the decrease of order during polymerization as drastically. The decrease in dichroic ratio during polymerization of 15, 19, and 11% was determined for mixtures **M−A₁A₂(50%)**, **M−A₁A₂(25%)** and **M−A₂**, respectively. Another possible cause for the decrease of the dichroic ratio upon polymerization is found in the fact that if the acrylate groups are too close to the central mesogenic units, polymer formation disrupts the high order of these central units. By replacing the hexyl spacers (series **A**) by undecyl spacers (series **B**) in the general structure, the acrylate groups are placed further away from the mesogenic units. It was expected that this change should minimize the effect of the photopolymerization of the acrylate groups on the order of the central
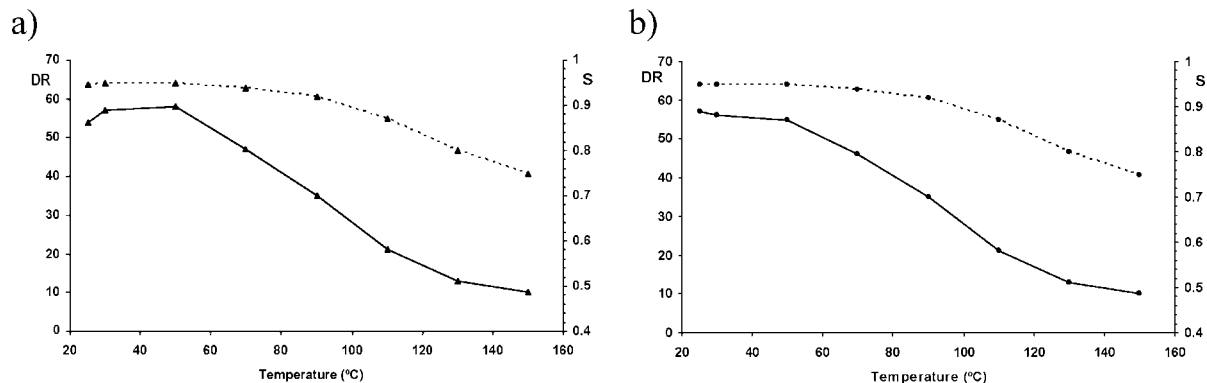
Figure 10. Thermal stability for the film prepared from **M−B₁B₂**(50%). (a) *DR* (▲, solid line) and *S* (▲, dotted line) data measured for the film on the heating process. (b) *DR* (●, solid line) and *S* (●, dotted line) data measured for the film on the cooling process.

mesogenic units and hence of the dichroic dye guests. A remarkable effect of the longer spacers is that the degree of order before polymerization is significantly higher. Dichroic ratios in absorption exceeding 90 are measured for **M−B₂** and **M−B₁B₂** mixtures. However, the decrease of the dichroic ratio during polymerization for these mixtures is larger to that observed for the short spacer analogue mixtures **M−A₂** and **M−A₁A₂**. As an example, a decrease in the dichroic ratio from 90 to 52 (42%) was observed for the dichroic mixture **M−B₁B₂(50%)**. Nevertheless, its final dichroic ratio after polymerization, exceeding 50, as well as an *S* parameter of 0.94 are the highest values measured, indicative of a high orientation degree of the dye within the network.

Oriented polymeric networks are expected to be temperature stable. The thermal stability of the oriented networks obtained from **M−B₁B₂(50%)** was tested. Figure 9 shows the order parameter for dye molecules in the polymer network obtained after photopolymerization as well as the order parameter for the same dye molecules in the unpolymerized binary mixture of polymerizable monomers as a function of temperature. The order parameter of the network was stable and practically constant, when the network was heated to temperatures up to 100 °C. At higher temperatures, a slight decrease of the order parameter, *S*, was observed. The dye order parameter in the polymerizable monomer mixture was high up to 90 °C. Below this temperature the mixture is in the smectic B phase. Above this temperature the mixture enters the smectic A phase where the order parameter is approximately 0.8. At 110 °C, the mixture has already past the nematic phase and has entered the isotropic phase with the corresponding order parameter $S = 0$.

Subsequently, the stability of the order after subsequent heating and cooling processes was investigated. For this purpose, the *DR* and *S* values of the liquid crystal cell containing the polymerized **M−B₁B₂(50%)** film were measured during several heating−cooling cycles. Figure 10 represents *DR* and *S* values measured during the second heating−cooling process. It can be seen that the order of the network slightly decreases during the heating process but is recovered upon cooling at room temperature. This occurs for subsequent heating−cooling cycles in a repetitive way.

Conclusions

Four series of compounds that contain polymerizable acrylate groups, exhibiting highly ordered smectic phases have been designed and synthesized. These compounds exhibit the desired combination of a highly ordered S_B phase, stable at room temperature and a highly fluidic nematic phase at elevated temperatures. Both liquid crystalline phases are requirements needed for their use in efficient polarizers for liquid crystal displays.

Highly ordered liquid crystal matrixes have been prepared from these monomers and homogeneous dichroic mixtures have been prepared from monomers of series **A** or series **B** and dichroic dye G205. All mixtures show stable smectic B mesomorphic behavior in wide temperature interval, including room temperature. Orientated dichroic mixtures with a high degree of order have been produced upon alignment of the liquid crystalline S_B host by surface forces. The dichroic ratio (*DR*) and order parameter (*S*) of the mixtures were determined by polarized UV−vis spectroscopy. The highest dichroic ratios before photopolymerisation were measured for the mixtures of compounds with undecylene spacers between the mesogenic moiety and the acrylate groups. Upon photopolymerization of the dichroic mixtures a decrease in the dye order parameter is observed for all samples. The decrease is most pronounced for mixtures based on pure diacrylate monomers. The best mixture is that of the network consisting of diacrylate **B₁** and one of the monoacrylates exhibiting the nematic phase, i.e., **B₂** or **B₃**. Especially, the mixture based on a 50/50 mixture of monomers **B₁** and **B₂** shows a very high degree of order before polymerization ($S = 0.98$) and relatively limited decrease of order parameter after photopolymerisation ($S = 0.94$). For samples based on this mixture, dichroic ratio values exceeding 50 after polymerization were obtained in a reproducible manner. The order parameter of the anisotropic networks was essentially stable with temperatures up to 100 °C. Further heating resulted in a loss of order; however, the order parameter was restored to its original value upon subsequent cooling to room temperature. The high dichroic ratios in combination with the temperature stability show that mixtures of these compounds have potential use for polarizers in liquid crystalline display applications.

Supporting Information Available: Synthetic procedures for the formation of the compounds. Mesomorphic properties data corresponding to the second heating and cooling scans. DSC thermograms. *DR* values measured for orientated cells at different temperatures. Photo-DSC studies. Study of the effect of the cis−trans isomerization of G205 in the dichroic dye measurements and thermal stability of the G205 dye (PDF). This material is available free of charge via the Internet at http://pubs. acs.org.

CM801133B